GRACE gravity analysis exploring climatic influences on mass changes in the Antarctic Peninsula

Abelardo Romero [1,2], Andreas Richter [1,2], Amilcar Juarez [1,2], Federico Suad Corbetta [1,2], Eric Marderwald [1,3], Pedro Granovsky [4], Thorben Döhne [5], Martin Horwath [5]

[1] Lab. MAGGIA, Universidad Nacional de La Plata, Argentina – (romeroabe, arichter, ajuarez, federicosc, emarderwald)@fcaglp.unlp.edu.ar
[2] Consejo Nacional de Investigaciones Científicas y Técnicas-CONICET, Argentina
[3] Estación Astronómica Río Grande, Argentina
[4] Facultad de Ciencias Astronómicas y Geofísicas, Universidad Nacional de La Plata, Argentina – pedrog@fcaglp.unlp.edu.ar
[5] Institut für Planetare Geodäsie, Technische Universität Dresden, Germany – (thorben.doehne, martin.horwat)@tu-dresden.de

Keywords: Antarctica, Satellite Gravimetry, Ice-Mass Balance

ABSTRACT:

Antarctic ice-mass balance is key to project sea-level changes, to assess future shifts in the global water cycle and ocean circulation, and to predict the fate of the White Continent. The ice mass of the Antarctic Peninsula is sensitive to the atmospheric and ocean circulation. The geographical conditions pose a challenge for modelling surface mass balance in this area. We use GRACE and GRACE Follow-On satellite gravimetry to derive a mass variation time series for the Antarctic peninsula region 2002-2024. We investigate whether these mass variations correlate with a surface mass balance model or with global climate indexes. Our analysis indicates a mass loss over two decades, mainly due to a period of enhanced mass-loss rate between 2007 and 2015. Our results suggest that interannual mass variations are primarily controlled by the surface mass balance which is influenced by the El Niño-Southern Oscillation phenomenon.

1 Introduction

Antarctic ice-mass balance is key to project sea-level changes, to assess future shifts in the global water cycle and ocean circulation, and to predict the fate of the White Continent. The ice-mass balance is composed of the surface mass balance (SMB), the basal mass balance and dynamic changes of the ice-mass flux across the grounding line. In a steady state the mass gain by the cumulated SMB (cSMB) is counterbalanced by the ice-mass loss implied by the glacier flux into the floating ice shelves, glacier tongues or iceberg calving and the, usually much smaller, basal mass balance. The SMB varies intensely on time scales of months to decades, and spatially over Antarctica as a consequence of a complex interplay between accumulation, transport and ablation. These processes respond to patterns and changes of the atmospheric and oceanic circulations which may extend far beyond Antarctica.

Antarctic ice-mass balance is usually estimated on continental scale, comprising the entire Antarctic Ice Sheet (AIS) and peripheral glaciers, such as those along the Antarctic Peninsula (Otosaka et al. 2022). The primary techniques employed in these continental estimates are satellite gravimetry (e.g., Groh & Horwath 2021; Fig. 1b), satellite altimetry (e.g., Schröder et al. 2019; Kappelsberger et al. 2024) or model-based input-output computations (e.g., Rignot et al. 2019). Integrated over entire Antarctica, they indicate a sustained ice-mass loss throughout the last three decades. While the ice mass in East Antarctica (1992-2022: +3 Gt/a; Otosaka et al. 2022) and the Antarctic Peninsula (-13 Gt/a) is not far from balance, the negative continental balance (-92 Gt/a) is essentially due to a dramatic ice-mass loss in West Antarctica (-82 Gt/a), focalized in the Amundsen Sea Embayment ("ASE" in Fig. 1b). There, changes in the ocean circulation, promoting the influx of warm circumpolar deep water, have increased the basal melting of the ice shelves at the termini of the main glaciers draining into the Amundsen Sea, especially the Pine Island and Thwaites glaciers (Turner et al. 2017). The reduction in ice-shelf buttressing has been causing an acceleration of the glaciers' ice flux and thus a dynamic downwasting (Bevan et al. 2024; Shepherd et al. 2019).

Compared to the AIS covering East and West Antarctica, the Antarctic Peninsula poses particular challenges for the quantification of ice-mass changes. The topography, finely structured by mountain ranges, bays and islands, fragments the ice into many individual glaciers and small drainage basins (Fig. 1a). This fragmentation and the steep mountain topography complicate the application of radar satellite altimetry (Schröder et al. 2019). The narrow shape of the peninsula, elongated in N-S direction aligned with primary uncertainty effects, is a challenge for the low spatial resolution provided by satellite gravimetry. In some parts of the peninsula, hydrological processes can contribute to the observable total mass change. The exposed position makes the peninsula region especially sensitive to the ocean and the atmosphere, including changes in the extrapolar circulation. The circulation has to be reproduced with high resolution by regional climate models in order to derive accurate SMB estimates. Furthermore, the peninsula is surrounded by numerous ice shelves. Major ice shelf disintegration events during the last decades have affected the flow dynamics and mass balance of the glaciers (Scambos et al. 2004; Rignot et al. 2004; Schannwell et al. 2018).

Some of the continental ice-mass balance estimates present also individual results for the Antarctic Peninsula, besides the West Antarctic Ice Sheet, East Antarctic Ice Sheet and individual drainage basins. However, methods successfully employed to quantify AIS mass changes from satellite gravimetry products, such as the "taylored sensitivity kernel" approach (Groh & Horwath 2021; Döhne et al. 2023), are

designed for continental scales and hardly able to account for the specific conditions of the peninsula. Owing to the pecularities of the region, previous ice-mass change estimates focussed on the Antarctic Peninsula used to employ different techniques than those available for continental studies (e.g., Seehaus et al. 2023).

Here we use GRACE and GRACE Follow-On satellite gravimetry data to derive an ice-mass change time series of the peninsula region (61-76°S, 55-80°W, except areas corresponding to ocean or ice shelves) from April 2002 through April 2024. Based on this new, regionalized time series we explore potential drivers of the observed mass changes, with an emphasis on interannual variations. Is the ice-mass change in the Antarctic Peninsula a consequence of changes in ice-flow dynamics governed by the ocean's interaction with the base of the ice shelves, as in the Amundsen Sea Embayment? Or is it rather controlled by the SMB? Are there global climatic patterns or teleconnections which impact the interannual ice-mass changes in the peninsula region, either via SMB, ice-shelf break-up, or ocean warming?

2 Methods

2.1 Determination of regional mass changes

We use Level-2 GRACE (2002-2017) and GRACE Follow-On (since 2018) satellite gravimetry products provided by ITSG (Mayer-Gürr et al. 2018) which consist of monthly gravity field solutions expressed in Stokes coefficients up to spherical harmonic degree and order 120. The combined time series of both missions is henceforth referred to as GRACE(FO). We discard the last published GRACE solutions (after January 2017) because of the reported data quality degradation. From each monthly coefficient set a global grid of surface density (i.e., equivalent water height) with a resolution of 0.75° is derived. The downward continuation of the space gravity data implied in this step amplifies the observational noise and causes the striping effect typical for unfiltered GRACE data representations. These noise effects can be reduced by filtering (Kusche et al. 2009) or by integration over a sufficiently large area or time span. We apply a temporal integration through the determination of mean rates (Fig. 2a) and amplitudes of the annual cycle (Fig. 2b) of the surface density variations in our area of interest.

In addition we integrate, for each monthly solution, the surface density within the on-land ice areas of the Antarctic Peninsula. For this purpose, a mask is constructed based on the SCAR Antarctic Digital Database (Gerrish et al. 2024) which assigns a weight to each surface density grid bin according to its areal contribution to the continental ice in the region of interest. In this way, the average surface density change is derived for each month, excluding floating ice shelves and ocean areas.

Our approach implies two major simplifications. First, no correction for leakage effects is applied. Leakage describes the blending of the sought gravity signal within the study region with mass-change effects in surrounding areas. In our case, leakage is primarily expected from ocean mass changes to either side of the Antarctic Peninsula. In terms of mass-change rate, models predict a decreasing ocean mass close to the Antarctic coasts. Thus, the gravity signal leaking into the peninsula area is negative, leading to an overestimation of the mass-loss rate. The second simplification is that we do not correct the gravity data for the effect of glacial isostatic adjustment (GIA). Mass displacements in the Earth’s interior in response to ice mass wasting in the past cause a progressive increase in gravity. Thus, our omission of this correction implies an underestimation of the mass-loss rates derived from GRACE.

2.2 Correlation with time series of SMB and climate indexes

In an attempt to identify the principal cause of the surface density variation observed by GRACE(FO), according to the questions formulated in the Introduction, we analyze time series of the SMB provided by the regional climate model RACMO2.3p (Van Wessem et al. 2016; Fig. 3b) and the El Niño-Southern Oscillation (ENSO; Hamlington et al. 2019; Fig. 3c) and Southern Annular Mode (SAM; Marshall 2003; Fig. 3d) climate indexes.

The RACMO model provides, for the peninsula region, monthly surface ice-mass balance time series on a fine mesh (5.5 km resolution). We use the spatial mask applied already to the GRACE(FO) surface density grid to derive, for each month, the mean SMB over the continental ice areas of the Antarctic Peninsula. The mass changes observed by GRACE(FO) are the result of the cumulative effect of the SMB variation. Therefore, the monthly SMB time series is cumulated, starting at the onset of the GRACE(FO) record, prior to its comparison with the mass-change time series. Since the monthly SMB is always positive, the cumulated SMB is monotonously increasing (Fig. 4a), compensating the ice-mass discharge across the grounding line (and the basal mass balance). As we focus here on interannual variations, and since the total ice-mass discharge along the coasts of the peninsula is difficult to quantify with the necessary accuracy, the time series of both GRACE-derived mass variation and cumulated SMB are de-trended by subtracting the linear temporal change of the corresponding time series (black line in Fig. 4a). The normalized, de-trended time series are then comparable and can be interpreted in terms of their correlation (Fig. 5). King et al. (2023) suggest to proceed in the same way with climate index time series in quest of correlation with mass variations derived from GRACE(-FO): The climate index time series are cumulated throughout the observation period and subsequently de-trended. We apply this procedure to the ENSO (Fig. 4b) and SAM (Fig. 4c) time series.

3 Results

The map of the mass-change rates derived from GRACE(FO) satellite gravimetry data (Fig. 2a) shows negative values along the entire Antarctic Peninsula, resulting in a total mass-change rate of -1 Gt/a (2002-2024). The intensity of this mass loss increases from north to south. The South Shetland Islands show a close-to-zero mass change, and also across the Bransfield Strait, at the northern tip of the peninsula, the mass loss is small. The largest mass-loss rates, reaching almost -3 kg m^{-2} a^{-1}, are found in the south-western corner of our study area. This area might be affected by signal leakage of intense ice-mass loss in the Amundsen Sea Embayment, not corrected in our estimate. The mean amplitudes of the annual mass cycle show a more heterogeneous pattern (Fig. 2b). Large seasonal mass variations are found, as expected, in the northern part of the peninsula, the area most exposed to atmospheric and ocean circulation. The patchy amplitude pattern might be affected by residual striping effects.

Figure 3a presents the time series of surface density variations, averaged over the on-land ice areas of the peninsula, derived from our GRACE(FO) analysis. It documents a mass loss over two decades, but with varying intensity: Between 2002 and 2007, and again since 2018 until early 2024, the surface density has remained almost constant. Between 2007 and 2015, an intense mass loss is observed.

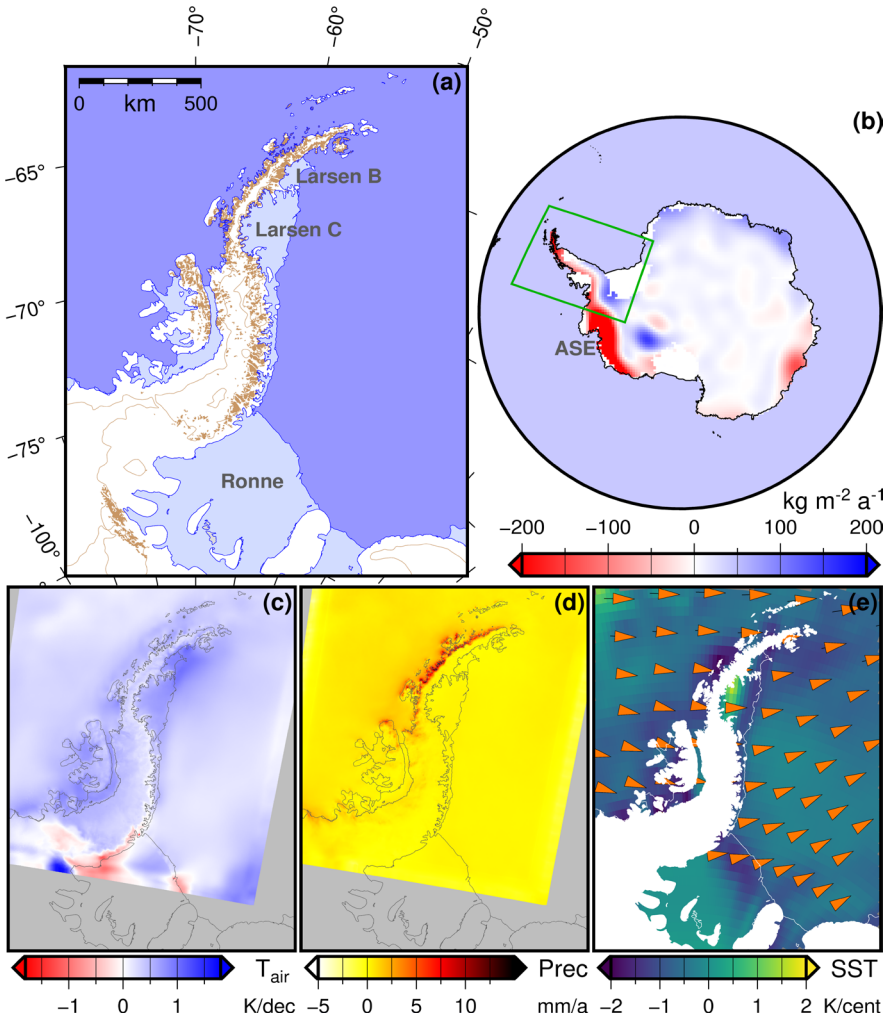

Figure 1. Maps of the region under investigation. (a) Topographic map of the Antarctic Peninsula region. Major ice shelves mentioned in the text are indicated. (b) Map of Antarctica. Green box shows the extent of map (a). Colors show the linear mass change rate 2002-2024 derived by Groh & Horwath (2021) from GRACE(FO) data. ASE: Amundsen Sea Embayment. (c) Air temperature (at 2 m) change rate 2000-2023 according to the RACMO 2.3p regional climate model (van Wessem et al. 2016) in Kelvin per decade. (d) Precipitation change rate 2000-2023 according to the RACMO 2.3p regional climate model (van Wessem et al. 2016) in millimeter water equivalent per year. (e) Sea surface temperature change rate 2000-2023 derived from the monthly mean values provided by NOAA (2024). Orange vectors indicate mean wind direction and speed at 500 hPa level 2000-2023 according to the RACMO 2.3p regional climate model (van Wessem et al. 2016).

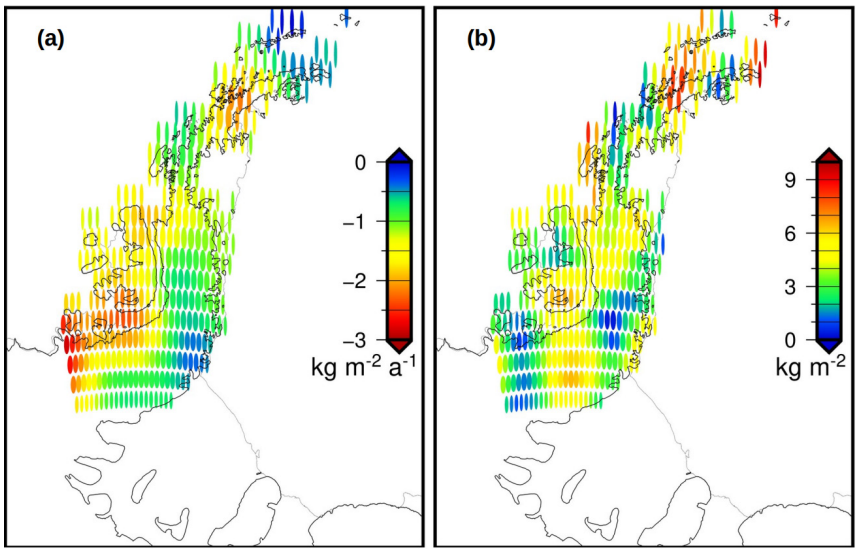

Figure 2. Maps of the Antarctic Peninsula showing mass changes derived from GRACE(Follow-On) and expressed as surface density. (a) Mass change rates 2002-2024 (b) Seasonal mass variations: amplitude of the mean annual cycle

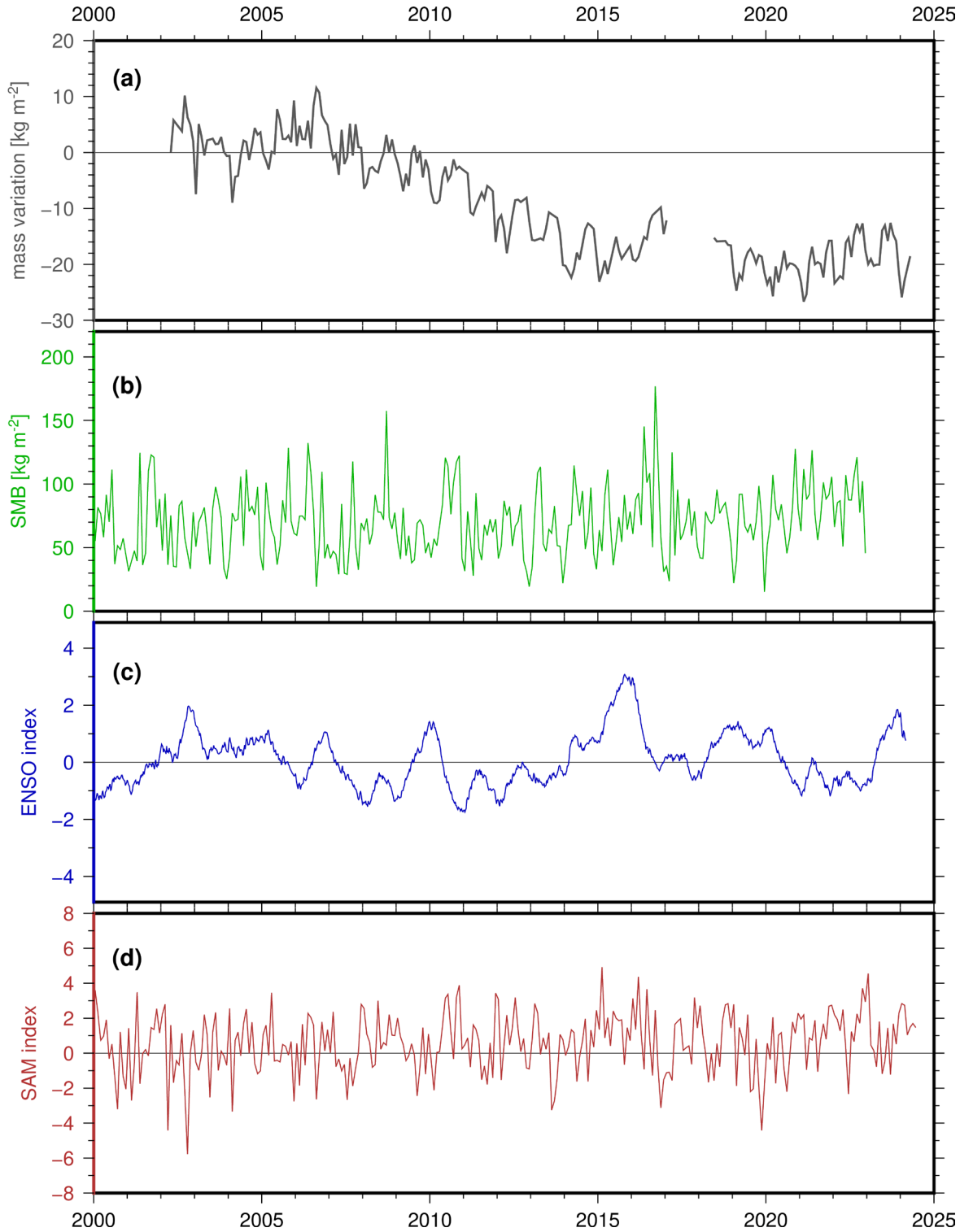

Figure 3. Time series available for the present analysis. (a) Surface mass density, derived from GRACE(FO) data, averaged over the continental ice area of the Antarctic Peninsula. (b) Surface mass balance, according to the regional climate model RACMO2.3p (Van Wessem et al. 2016), averaged over the continental ice area of the Antarctic Peninsula. (c) El Niño-Southern Oscillation index according to JPL (Hamlington et al. 2019) (d) Southern Annular Mode index (Marshall, 2003)

From 2015 until early 2017, the surface density has slightly increased. This decadal pattern is superimposed by the seasonal mass variation. The mean annual mass variation cycle is characterized by positive mass anomalies during austral winter (June through November) and a sharp drop during austral summer with a mass minimum in March.

The raw time series of the ENSO (Fig. 3c) and SAM (Fig. 3d) indexes show, as expected, no correlation with the observed mass variations (Fig. 3a) and regional mean SMB (Fig. 3b). The averanged SMB is positive throughout the GRACE(FO) period with a mean monthly SMB of +70 kg m^{-2} a^{-1}. Also the SMB is characterized by a mean annual cycle which precedes that of the mass variations by 2.5 months (SMB minimum in January). In order to separate the impact of long-term processes, such as ice discharge, from possible driving climate signals, we compare in Fig. 5 the de-trended and

(blue shaded periods in Fig. 5) tend to promote an increase in SMB and mass. This relationship can be established for four out of the seven events during the GARCE(FO) period. A relationship with El Niño phases is not as clear. Three of six El Niño events (red) could be associated with some decrease in SMB, but there is no evident relation with the interannual mass variations observed by GRACE(FO). The comparison of the normalized, de-trended time series of cumulative ENSO with GRACE-derived mass variation in Fig. 6 reveals a moderate correlation, with the mass time series lagging

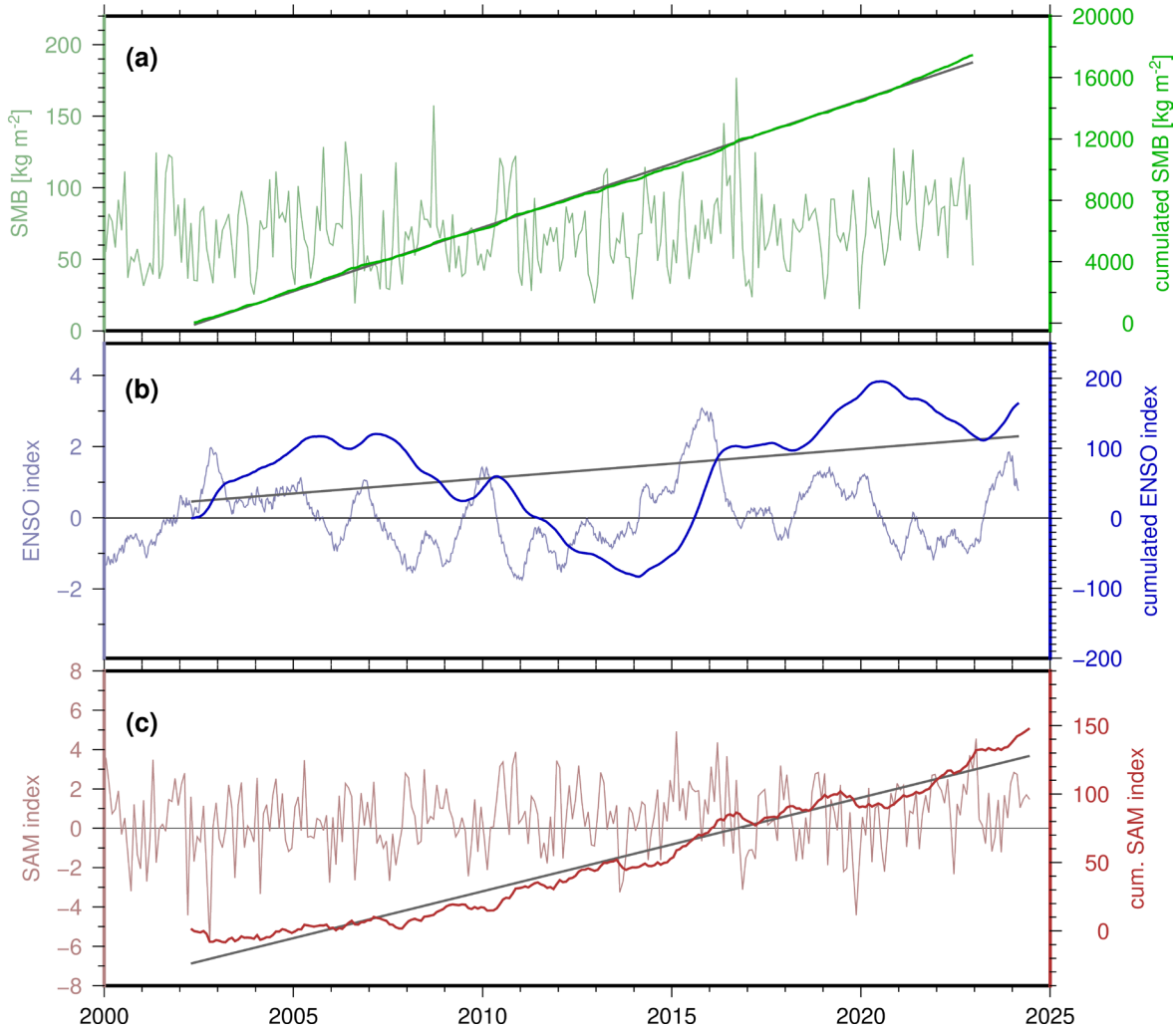

Figure 4. Processing of the time series of climatic variables and indexes for their comparison with the GRACE-derived mass change time series. (a) Surface mass balance (SMB) according to the regional climate model RACMO2.3p (Van Wessem et al. 2016), averaged over the continental ice area of the Antarctic Peninsula. Thin, pale green curve: original time series of mor SMB (identical to Fig. 3b); bright green: cumulated SMB; black line: linear trend fitted to the cumulated SMB. (b) El Niño-Southern Oscillation (ENSO) index (Hamlington et al. 2019). Thin, pale blue curve: original ENSO index time series (identical to Fig. 3c); thick blue: cumulated ENSO index; black line: linear trend fitted to the cumulated ENSO index. (c) Southern Annular Mode (SAM) index (Marshall, 2003). Thin, pale red curve: original SAM index time series (identical to Fig. 3d); t red: cumulated SAM index; black line: linear trend fitted to the cumulated SAM index.

normalized time series of GRACE(FO)-derived mass variation and cSMB. Both time series show a statistically significant correlation with a Pearson coefficient of 0.60. In particular, the cSMB time series reproduces coherently the major inflection points that mark the observed mass change evolution (2007, 2015, 2017).

The comparison of the SMB and mass variation time series with the different ENSO phases indicates that La Niña events

approximately 11 months behind the ENSO index. We do not find an interpretable correlation between the SAM index (Fig. 6, red) and our mass variation time series.

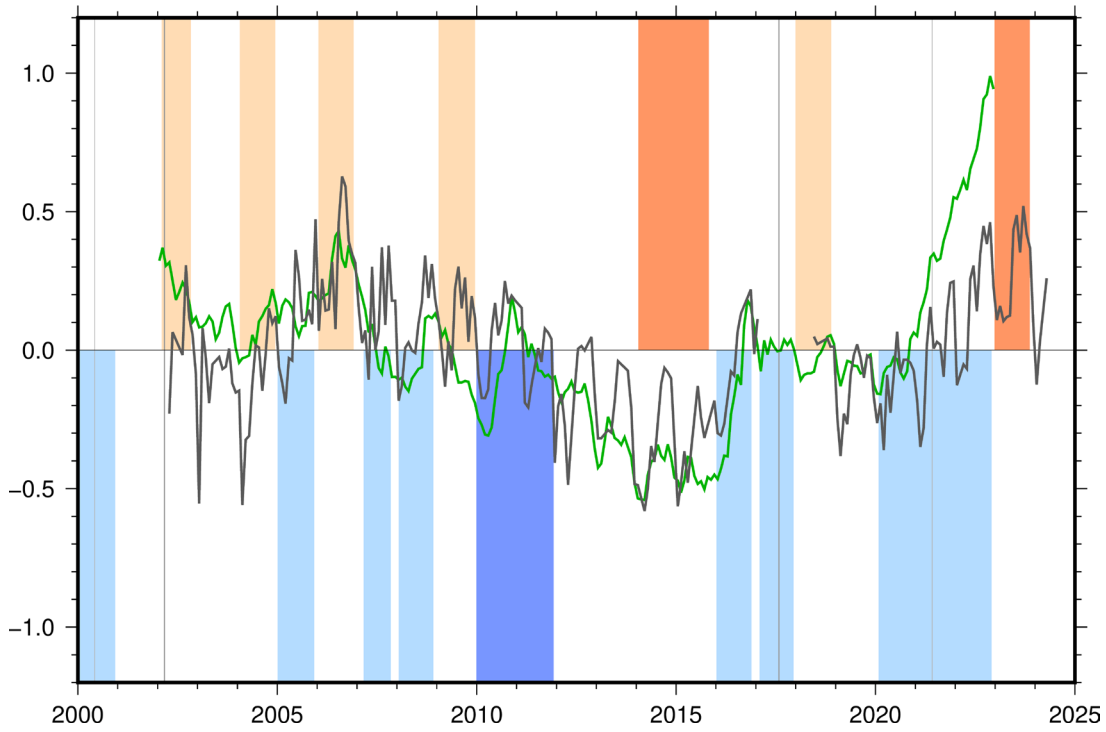

Figure 5. Comparison of the de-trended and normalized time series of the mass variations derived from GRACE(FO) (grey) and the cumulative surface mass balance according to the RACMO2.3p climate model (Van Wessem et al. 2016; green). I shaded periods indicate the duration of El Niño events, highlighting the severe events of 2014-2016 and 2023-2024. Blue shaded periods correspond to La Niña events, emphasizing the strong 2010-2012 event. Vertical grey lines indicate the da of major ice-shelf disintegrations events: Larsen-B collapse (2002) and Larsen-C major calving event (2017) in dark grey; large iceberg break-up events from Ronne Ice Shelf (2000, 2021) in light grey.

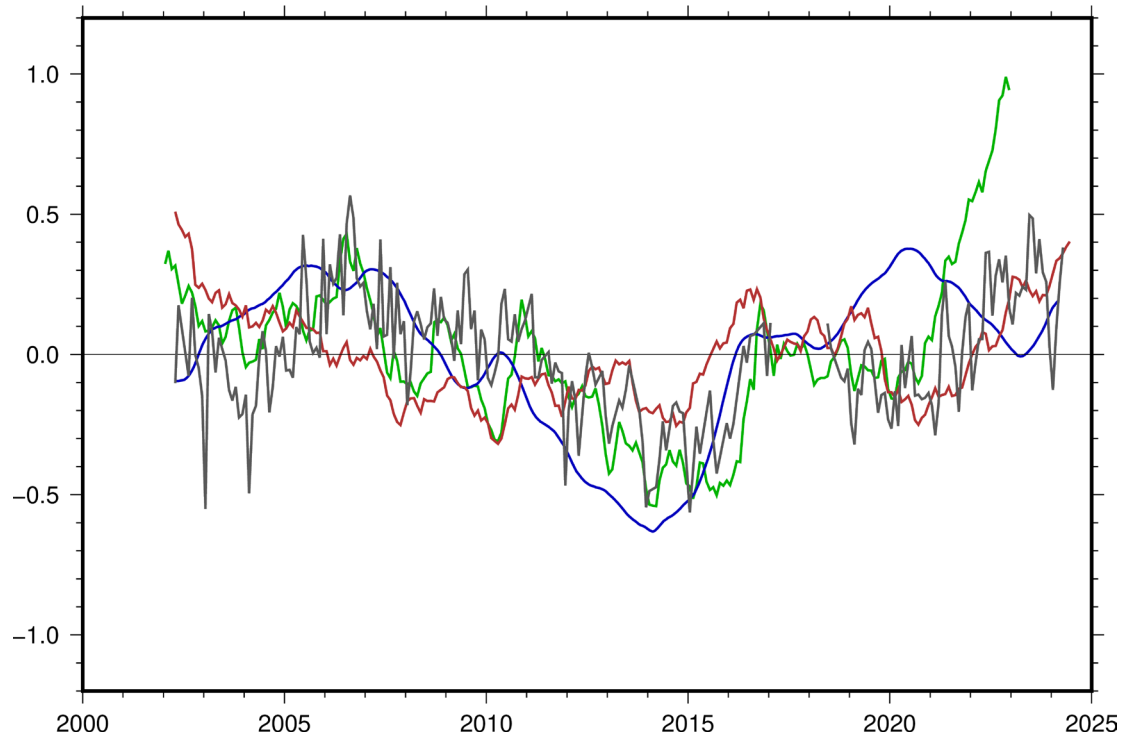

Figure 6. Comparison of the de-trended, normalized time series of mass variations derived from GRACE(FO) (grey) with cumulated, de-trended and normalized time series of: surface mass balance (green; Van Wessem et al. 2016), El Niño-South Oscillation index (blue; Hamlington et al. 2019), and Southern Annular Mode index (red; Marshall 2023)

4 Discussion

Our total mass change rate of -1 Gt/a indicates a slower mass loss than most continental-scale (Groh & Horwath 2021, 2002-2024: -20 Gt/a; Otosaka et al. 2023, reconciled estimate 1992-2020: -13 Gt/a) and regional (Seehaus et al. 2023, northern Antarctic Peninsula Ice Sheet 2013-2017: -24 Gt/a) estimates, but falls within the spread of the individual solutions and derived uncertainty presented by Otosaka et al. (2023; their Fig. 2c). Reasons for this lower rate value are, besides differing spatial and temporal integration boundaries, methodical differences in the GRACE(FO) satellite gravimetry data processing, especially our omission of the GIA correction. Since GIA effects are expected to be linear throughout the GRACE operation period, this omission should not affect significantly the interannual variability on which the present work focusses. Indeed, our mass variation time series is consistent with the one presented by King et al. (2023), in particular regarding the major inflection points (2007, 2015, 2017). The spatial pattern of the mass change rate (Fig. 2a) is in agreement with previous works. In particular, the low mass-loss rates observed at the northern tip of the peninsula and the South Shetland islands agree with local studies in this area (Shahateet et al. 2021; Oliva et al. 2017) which relate observed glacier changes with a cooling trend in the early 2000s (Fig. 1 c). In addition, the generally negative mass balance is damped along the NW coast of the peninsula by the precipitation increase (Fig. 1 d) due to enhanced moisture transport from the west (Fig. 1 e).

Sea-surface temperature change rates derived from monthly mean global grids provided by NOAA (2024) show a generally stable ocean temperature throughout the peninsula region (Fig. 1 e), except for a hotspot of intense warming centered at Mill Inlet (Larsen C ice shelf; +0.2 K per decade) and a locus of cooling at the opposite side of the peninsula (east of Renaud Island; -0.2 K per decade). Without delving into a detailed assessment of the reliability of these sea-surface temperature data, it is generally accepted that ocean processes contributed to the collapse of the Larsen ice shelves. However, the ice-ocean interaction is not conceded a role as dominant as in the Amundsen Sea. The Larsen ice-shelf destabilization is rather related with hydrofracturing by surface ponds (Scambos et al. 2009) and ice-melange thinning (Larour et al. 2021) associated with warm atmospheric anomalies attributed to La Niña and Southern Annular Mode teleconnections (Wang et al. 2023).

The analysis of the non-linear, interannual mass variations might serve us as a key to identify the primary process driving the ice-mass change in the peninsula. If the mass loss were primarily due to dynamic downwasting following a reduction in ice-shelf buttressing, like in the case of the Amundsen Sea Embayment, we would expect some correlation of the inflection points of the regional ice-mass evolution with major ice-shelf disintegration events. However, the timing of the major changes in mass-loss rate do not suggest a straightforward relationship with ice-shelf disintegration (Fig. 5, vertical grey lines). The disintegration of Larsen-B (2002) preceded the onset of the accelerated mass loss (2007) by five years. While some delay in the ice-mass response is expected, our time series provides no basis for a causal relation of the speed-up of ice-mass loss with the Larsen-B ice shelf. No similar acceleration in mass loss is observed within six years of the major calving event on the Larsen-C ice shelf (2017). This distinction may partly explain the lack of an acceleration, as the calving event, although significant, did not result in a collapse of the Larsen-C ice shelf, which remains at risk of disintegration (Gilbert et al. 2022). Moreover, a mass-loss history governed by ice-flux dynamics would not be expected to correlate significantly with SMB.

The moderate, delayed correlation of the observed mass variation with the cumulated ENSO index has also been established by previous works (Sasgen et al. 2010; King et al. 2023). In particular, our estimated lag of 11 months between mass and ENSO variation coincides very well with the 10 months delay derived by Sasgen et al. (2010). Nevertheless, this correlation does not elucidate the mechanism which links the mass change with the climatic teleconnections. Do climate patterns like ENSO drive ice-shelf disintegration, as suggested by Wang et al. (2023), which accelerate dynamic ice discharge? Do large-scale climate patterns control transient, local sea-surface warming at the base of ice shelves and glacier tongues, enhancing ice flux? The statistically significant correlation we find between cSMB and the observed mass variation clarifies the mechanism that relates our GRACE time series with ENSO. It suggests that mass variations of the Antarctic Peninsula are primarily controlled by the SMB which, in turn, is affected by ENSO.

The fact that we do not find an evident correlation with the SAM index does not mean that this climate pattern has no effect on the ice mass in the peninsula region. King et al. (2023) show, over entire Antarctica, that a multivariate regression including both ENSO and SAM has to be employed to explain the observed mass variation. Our results suggest that in the peninsula region the ENSO index is more effective than the SAM. But a more sophisticated analysis in the future might establish also a significant contribution from the SAM.

5 Conclusion

Our results suggest that mass variations of the Antarctic Peninsula are primarily controlled by the SMB. The SMB is influenced by ENSO, mainly during the La Niña phase. The RACMO2.3p model (Van Wessem et al. 2016) reproduces multi-annual SMB changes consistently with mass variations observed with GRACE(FO), also during La Niña events. Thus, our GRACE(FO) results can be interpreted as a qualitative validation of this regional climate model. Future work will priorize the improvement of our regional mass variation time series. Besides the application of a GIA correction, we will employ the inversion method proposed by Richter et al. (2019) in order to suppress leakage and striping effects and to increase the spatial resolution.

References

Bevan, S., Cornford, S., Gilbert, L., Otosaka, I., Martin, D., Surawy-Stepney, T. (2023). Amundsen Sea Embayment ice-sheet mass-loss predictions to 2050 calibrated using observations of velocity and elevation change. Journal of Glaciology. doi:10.1017/jog.2023.57.

Döhne, T., Horwath, M., Groh, A., Buchta, E. (2023). The sensitivity kernel perspective on GRACE mass change estimates. J Geod 97(11). doi:10.1007/s00190-022-01697-8.

Gerrish, L., Ireland, L., Fretwell, P., & Cooper, P. (2024). High resolution vector polylines of the Antarctic coastline (7.9). UK Polar Data Centre, NERC. doi:10.5285/45c3cc90-098b-45e3-a809-16b80eed4ec2.

Gilbert, E., Orr, A., Renfrew, I. A., King, J. C., & Lachlan-Cope, T. (2022). A 20-year study of melt processes over Larsen C ice shelf using a high-resolution regional atmospheric model: 2. Drivers of surface melting. Journal of Geophysical Research: Atmospheres, 127, e2021JD036012. https://doi.org/10.1029/2021JD036012

Groh, A. & Horwath, M. (2021). Antarctic Ice Mass Change Products from GRACE/GRACE-FO Using Tailored Sensitivity Kernels. Remote Sensing 13(9):1736. doi:10.3390/rs13091736.

Hamlington, B. D., Cheon, S. H., Piecuch, C. G., Karnauskas, K. B., Thompson, P. R., Kim, K.-Y., et al. (2019). The dominant global modes of recent internal sea level variability. Journal of Geophysical Research: Oceans 124:2750-2768. doi:0.1029/2018JC014635.

Kappelsberger, M. T., Horwath, M., Buchta, E., Willen, M. O., Schröder, L., Veldhuijsen, S. B. M., Kuipers Munneke, P., van den Broeke, M. R. (2024). How well can satellite altimetry and firn models resolve Antarctic firn thickness variations? The Cryosphere 18:4355-4378, doi:10.5194/tc-18-4355-2024.

King, M.A., Lyu, K., Zhang, X. (2023). Climate variability a key driver of recent Antarctic ice-mass change. Nat. Geosci. 16:1128-1135, doi:10.1038/s41561-023-01317-w.

Kusche, J., Schmidt, R., Petrovic, S., Rietbroek, R. (2009). Decorrelated GRACE time-variable gravity solutions by GFZ, and their validation using a hydrological model. Journal of Geodesy 83(9):903-913. doi:10.1007/s00190-009-0308-3.

Larour, E., Rignot, E., Poinelli, M., Scheuchl, B. (2021). Physical processes controlling the rifting of Larsen C Ice Shelf, Antarctica, prior to the calving of iceberg A68. Proc Natl Acad Sci USA 118(40):e2105080118. doi:10.1073/pnas.2105080118.

Marshall, G.J. (2003). Trends in the Southern Annular Mode from observations and reanalyses. Journal of Climate, 16:4134-4143. doi:10.1175/1520-0442(2003)016<4134:TITSAM>2.0.CO;2.

Mayer-Gürr, T., Behzadpur, S., Ellmer, M., Kvas, A., Klinger, B., Strasser, S., Zehentner, N. (2018). ITSG-Grace2018 - Monthly, Daily and Static Gravity Field Solutions from GRACE. GFZ Data Services. doi:10.5880/ICGEM.2018.003.

NOAA (2024). National Oceanic and Atmospheric Administration (USA), THREDDS Data Server. URL: https://psl.noaa.gov/thredds/catalog/Datasets/noaa.oisst.v2/catalog.html?dataset=Datasets/noaa.oisst.v2/sst.oisst.mon.mean.1982.nc (last access: 18/10/2024).

Oliva, M., Navarro, F., Hrbáček, F., Hernández, A., Nývlt, D., Pereira, P., Ruiz-Fernández, J., Trigo, R. (2017). Recent regional climate cooling on the Antarctic Peninsula and associated impacts on the cryosphere. Sci. Total Environ 580:210-223. doi:10.1016/j.scitotenv.2016.12.030.

Otosaka, I. N., Shepherd, A., Ivins, E. R., Schlegel, N.-J., Amory, C., van den Broeke, M. R., Horwath, M. et al. (2022). Mass balance of the Greenland and Antarctic ice sheets from 1992 to 2020. Earth Syst. Sci. Data 15:1597-1616. doi:10.5194/essd-15-1597-2023.

Richter, A., Groh, A., Horwath, M., Ivins, E., Marderwald, E., Hormaechea, J.L., Perdomo, R., Dietrich, R. (2019). The Rapid and Steady Mass Loss of the Patagonian Icefields throughout the GRACE Era: 2002–2017. Remote Sensing 11(8):909. doi:10.3390/rs11080909.

Rignot, E., Casassa, G., Gogineni, P., Krabill, W., Rivera, A., Thomas, R. (2004). Accelerated ice discharge from the Antarctic Peninsula following the collapse of Larsen B ice shelf. Geophys. Res. Lett. 31:L18401, doi:10.1029/2004GL020697.

Rignot, E., Mouginot, J., Scheuchl, B., Morlighem, M. (2019). Four decades of Antarctic Ice Sheet mass balance from 1979–2017. Proceedings of the National Academy of Sciences USA 116(4):1095-1103. doi:10.1073/pnas.1812883116.

Sasgen, I., Dobslaw, H., Martinec, Z., Thomas, M. (2010). Satellite gravimetry observation of Antarctic snow accumulation related to ENSO. Earth and Planetary Science Letters 299(3-4):352-358, doi:10.1016/j.epsl.2010.09.015.

Scambos, T.A., Bohlander, J.A., Shuman, C.A., Skvarca, P. (2004). Glacier acceleration and thinning after ice shelf collapse in the Larsen B embayment, Antarctica. Geophys. Res. Lett. 31:L18402. doi:10.1029/2004GL020670.

Scambos, T., Fricker, H.A., Liu, C.C., Bohlander, J., Fastook, J., Sargent, A., Massom, R., Wu, A.-M. (2009.) Ice shelf disintegration by plate bending and hydro-fracture: Satellite observations and model results of the 2008 Wilkins ice shelf break-ups. Earth and Planetary Science Letters 280(1-4):51-60. doi:10.1016/j.epsl.2008.12.027.

Schannwell, C., Cornford, S., Pollard, D., Barrand, N. E. (2018). Dynamic response of Antarctic Peninsula Ice Sheet to potential collapse of Larsen C and George VI ice shelves. The Cryosphere 12:2307-2326. doi:10.5194/tc-12-2307-2018.

Schröder, L., Horwath, M., Dietrich, R., Helm, V., van den Broeke, M., Ligtenberg, S. R. (2019). Four decades of Antarctic surface elevation changes from multi-mission satellite altimetry. The Cryosphere. 13:427-449. doi:10.5194/tc-13-427-2019.

Seehaus, T., Sommer, C., Dethinne, T., Malz, P. (2023). Mass changes of the northern Antarctic Peninsula Ice Sheet derived from repeat bi-static synthetic aperture radar acquisitions for the period 2013–2017. The Cryosphere 17:4629-4644. doi:10.5194/tc-17-4629-2023.

Shahateet, K., Seehaus, T., Navarro, F., Sommer, C., Braun, M. (2021). Geodetic Mass Balance of the South Shetland Islands Ice Caps, Antarctica, from Differencing TanDEM-X DEMs. Remote Sensing 13(17):3408, doi:10.3390/rs13173408.

Shepherd, A., Gilbert, L., Muir, A.S., Konrad, H., McMillan, M., Slater, T., et al. (2019). Trends in Antarctic Ice Sheet elevation and mass. Geophysical Research Letters 46:8174-8183. doi:10.1029/2019GL082182.

Turner, J., Orr, A., Gudmundsson, G.H., Jenkins, A., Bingham, R.G., Hillenbrand, C.-D., Bracegirdle, T.J. (2017). Atmosphere-ocean-ice interactions in the Amundsen Sea Embayment, West Antarctica. Rev. Geophys. 55:235-276, doi:10.1002/2016RG000532.

van Wessem, J.M., Ligtenberg, S.R.M., Reijmer, C.H., van de Berg, W.J., van den Broeke, M.R., Barrand, N.E., Thomas, E.R., Turner, J., Wuite, J., Scambos, T.A., van Meijgaard, E. (2016). The modelled surface mass balance of the Antarctic Peninsula at 5.5 km horizontal resolution. The Cryosphere 10:271-285. doi:10.5194/tc-10-271-2016.

Wang, S., Liu, H., Alley, R.B., Jezek, K., Alexander, P., Alley, K.E., Huang, Z., Wang, L. (2023). Multidecadal pre- and post-collapse dynamics of the northern Larsen Ice Shelf. Earth and Planetary Science Letters 609:118077, doi:10.1016/j.epsl.2023.118077.